V European Conference on Computational Fluid Dynamics
ECCOMAS CFD 2010
J. C. F. Pereira and A. Sequeira (Eds)
Lisbon, Portugal, 14–17 June 2010

SIMULATIONS OF UPWARD FLAME SPREAD BY COUPLING A PYROLYSIS MODEL WITH A CFD CALCULATION

Pieter Rauwoens*, Joris Degroote, Shivanand Wasan, Jan Vierendeels, Bart Merci

Ghent University, Department of Flow, Heat and Combustion Mechanics
Sint-Pietersnieuwstraat 41, 9000 Gent, Belgium
{pieter.rauwoens, joris.degroote, shivanand.wasan, jan.vierendeels, bart.merci}@ugent.be

Key words: CFD, Pyrolysis, Flame Spread, Fire.

Abstract. *In simulations of developing fires in enclosures, a correct prediction of flame spread is crucial in the prediction of the fire growth rate. The simulation of this phenomenon requires two different kinds of solvers: one that deals with the solid phase, to determine the thermal degradation and volatile release (pyrolysis); a second one that calculates the combustion process in the flame formed by mixing of the volatiles with the ambient air. The processes in the solid and the gas phase require proper modeling. Moreover, an adequate coupling strategy at the interface between the solid and the gas phase is an important point of interest. The paper focuses on a method to successfully combine these two types of calculations. Two types of flame spread (upward and downward) demonstrate the possibilities of this approach. We conclude that the coupling between the two phases works fine, providing a mechanism of simulating flame spread with two different codes. It is found, however, that the prediction of the gas phase requires an appropriate choice of the CFD sub-models, particularly in case of upward flame spread. The impact of different turbulence models illustrates that totally different flame dynamics can be predicted.*

1 INTRODUCTION

In simulations of developing fires in enclosures, it is crucial to correctly predict the rate of flame spread over combustible surfaces. This phenomenon involves chemical reactions in the solid and the gas phase. In the solid phase, upon external heat input, the virgin material degrades at higher temperatures, releasing combustible volatiles. This pyrolysis process thus consumes an amount of heat and generates an amount of fuel. In the gas phase, these volatiles mix with the ambient air and a combustion reaction takes place, with the formation of a flame. This process thus provides an amount of heat and consumes an amount of fuel. The spread of a flame is controlled by the timescale of the mechanism described above. In order to correctly predict flame spread, both the solid and the gas phase require proper modeling. Moreover, an adequate coupling strategy at the interface between the solid and the gas phase is an important point of interest. In the present paper, we focus on the coupling strategy and describe the models invoked. It will appear that better models are needed if one wants to qualitatively study upward flame spread phenomena.

Two types of flame spread are intensively studied in literature. The driving mechanism is in both cases the heat input from the flame to the solid. In the case of upward flame spread, the heat transfer from the flame to the virgin material happens primarily by radiation. A correct prediction of flame height is therefore essential for the correct prediction of flame spread. The flame height prediction depends on the kinetics of the chemical reaction considered and to a greater extent, especially in the case of a turbulent flow, on the (turbulent) mixing between fuel and oxidizer. In the case of downward flame spread, the heat transfer between the flame and the virgin solid is established by gas phase conduction. Since the virgin material does not really see the flame, radiation can be neglected (cf. [1]).

From the above, it can be expected that downward flame spread simulations are not that dependent on models for radiation and soot, invoked in the gas phase. Therefore, particularly in laminar flows, they suit as the ideal test cases for checking the quality of the solid phase model and the coupling between the two phases. In practice, downward flame spread is not encountered that often and is far less severe in terms of fire hazards than upward flame spread, which happens a lot faster. Therefore, the future focus is on upward flame spread simulations. In this paper, we also show that the coupling strategy works fine for upward flame spread simulations, but, because of the gas phase models, the flame height is not correctly predicted. More precisely, as will be demonstrated further down, it is the position of the flame's leading edge that is wrongly predicted.

Upward flame spread simulations have mostly been performed with PMMA as solid material (e.g. [2]). Its properties are well known and much experimental work is available to validate the results. PMMA is categorized as a non-charring material: during the pyrolysis process, all virgin material transforms into volatiles. A charring material (pine wood for example) does not transform completely in volatiles, but leaves behind char, allowing for higher surface temperatures. The solid phase model has the property that it is a unified code that can handle both charring and non-charring materials. Upward flame spread simulations are performed on both types of materials.

2 SOLID PHASE MODEL

The solid phase is described by an enthalpy model. This means that one transport equation for static enthalpy is solved:

$$\frac{\partial \rho h}{\partial t} = -\frac{\partial \dot{q}''_{conv}}{\partial x} - \frac{\partial \dot{q}''_{cond}}{\partial x} \tag{1}$$

The enthalpy level changes because conduction takes place in the material and an amount of enthalpy is convected outwards with the volatile release. Conduction can be described in all directions by Fourier's law, whereas the model assumes that the transport of gases is perpendicular to the exposed surface. Pyrolysis is described as a phase change at the pyrolysis temperature T_{pyr} and requires an amount of heat Q_{pyr} per mass unit of volatiles produced.

Since we use a discretization of Eq. 1 on a fixed mesh, the temperature field is represented as a piecewise linear function (linear from node to node or from node to pyrolysis front location). If a piecewise constant temperature representation were to be used, as is standard in a finite volume formulation, the mass flow rate of volatiles would become discontinuous, which is not favorable for coupling with a CFD-code.

From the enthalpy, the temperature field and pyrolysis front location are reconstructed by expressing that

$$\rho h V = \int_{cell\ volume} \rho(x) h\big(T(x)\big).dx \tag{2}$$

and

$$\left(\rho_v - \rho_c\right)\frac{dx_{f,pyr}}{dt} Q_{pyr} = -k_c \left.\frac{\partial T}{\partial x}\right|_c + k_v \left.\frac{\partial T}{\partial x}\right|_v \tag{3}$$

Expression (3) states that the pyrolysis front is allowed to move, if more heat is provided than goes through by conduction. The amount of heat consumed during the pyrolysis process is related to Q_{pyr}: the generation of one unit of mass volatiles (at T_{pyr}) out of virgin material (at T_{pyr}), eventually leaving behind char (at T_{pyr}), consumes an amount of enthalpy equal to Q_{pyr} (fig. 1) In Eq. 2, h(T) consists of the sensible enthalpy and the formation enthalpy of virgin/char material. Indeed: it is assumed that the pyrolysis gases immediately leave the solid once they are formed. As such, they do not contribute in the determination of the enthalpy level of a grid cell in the solid. The relation between enthalpy and temperature for a pure component (in casu virgin or char) is expressed by means of the specific heat (fig. 2). Full details on the solution procedure can be found in [3,4].

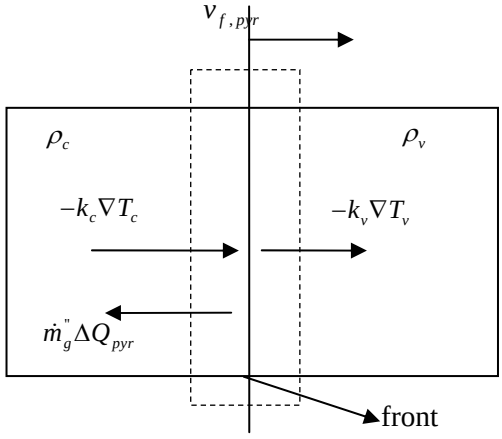

Figure 1: Mass and energy balance around the front (Eq. 3)

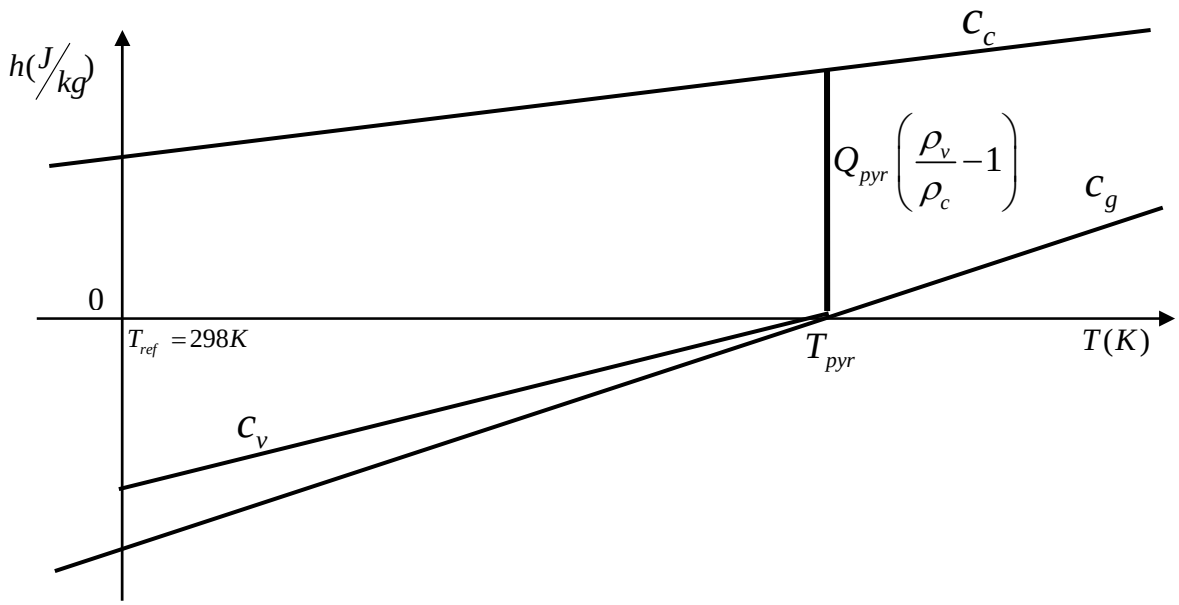

Figure 2: Relation between enthalpy and temperature for the different components: virgin material (v), char (c) and volatiles (g).

Generally speaking, the solid phase pyrolysis code can be seen as a black box solver, providing a solution for the solid phase in the form

$$(\dot{\mathbf{m}}''_{pyr}, \mathbf{T}_s) = S(\dot{\mathbf{q}}''_{in}) \tag{4}$$

with $\dot{\mathbf{m}}''_{pyr} = (\rho_c - \rho_v) d\mathbf{x}_{f,pyr}/dt$ the mass flow rate vector at the gas-solid interface and $\mathbf{T}_s$ the surface temperature vector. $\dot{\mathbf{q}}''_{in}$ is the incident heat flux vector, coming from the flame. Note that, for non-charring materials, the surface temperature cannot reach values higher than T_{pyr}. Also, in that case, $-k_c \partial T/\partial x|_c$ is replaced by $\dot{q}''_{in}$, since no char exists.

3 GAS PHASE MODEL

The gas phase is simulated with the commercial package Ansys Fluent. Conservation equations of mass, species mass fractions, momentum and energy are solved. In case of turbulent flows, two extra equations are solved (conservation of turbulent kinetic energy and turbulent dissipation rate). We describe some specific features of the sub models below.

Generally speaking, the gas phase CFD code can be seen as a black box solver, providing a solution for the gas phase in the form

$$(\dot{\mathbf{q}}''_{in}) = G(\dot{\mathbf{m}}''_{pyr}, \mathbf{T}_s) \tag{5}$$

3.1 Conservation equations

In general, the conservation equations of mass, momentum and energy take the form

$$\frac{\partial \rho\phi}{\partial t} + \frac{\partial \rho u_i \phi}{\partial x_i} = \frac{\partial}{\partial x_i}\left(\rho\Gamma \frac{\partial \phi}{\partial x_i}\right) + S \tag{6}$$

with ϕ equal to {1, u_x, u_y, h, Y_F, Y_{O2}, Y_{CO2}, Y_{H2O} }. The diffusivities are calculated as a function of the mixture, with constant thermal conductivity k=0.0454 W/m^{2}K and constant species diffusivity D=2.88e-5 m^2/s. Specific heat is calculated with a mixing law, and each component uses polynomial functions for specific heat as a function of temperature. Viscosity is calculated using Sutherland's Law for the different species.

If MMA is considered as a fuel, the same properties are given as air at that temperature, apart from the specific heat and the density. The specific heat of MMA is considered constant c_p=1183 J/kgK. All appearing species are treated as an incompressible ideal gas, which means that density is given by

$$\rho_\alpha = \frac{p_0 M_\alpha}{RT} \tag{7}$$

Source terms S include chemical source terms in species and energy equation and, if radiation is taken into account, a radiant heat source in the energy equation. In the momentum equation, gravity acts as a source term as well.

3.2 Chemical reactions

Chemistry is treated as a single-step reaction, depending on the fuel:

$$\begin{aligned} MMA + 6O_2 &\rightarrow 5CO_2 + 4H_2O \\ C_3H_8 + 5O_2 &\rightarrow 3CO_2 + 4H_2O \end{aligned} \tag{8}$$

The chemical source term in laminar flow calculation is determined by the Arrhenius expression

$$S_{MMA} = -A\rho^2 Y_{MMA} Y_{O_2} \exp(T_{act}/T) \tag{9}$$

with pre-exponential factor A=5.928e+9 m^3/kgs and activation temperature T_{act} = 1.07e+4 K . The heat of combustion of MMA is taken as Δh=25.9 MJ/kg [5].

In turbulent flows, the reaction is not controlled by the chemical kinetics. It rather is the mixing between fuel and oxidizer that controls the reaction rate. We use the Eddy Break-Up model to determine the reaction as a function of the turbulent mixing time scale:

$$S_{MMA} = -4\rho \frac{k}{\varepsilon} \min(Y_{MMA}, Y_{O_2}/f) \tag{10}$$

with f=1.92 the stoichiometric oxygen to fuel mass ratio. In case of propane as a fuel, Eq. 10 remains similar, with a different value for f.

3.3 Turbulence

Unless mentioned otherwise, turbulence is modeled with the RNG k-ε model. The turbulence model includes two extra transport equations, for the turbulent kinetic energy *k* and the turbulent dissipation rate ε. Extra terms are introduced in the equations to include the effect of buoyancy on turbulence generation. At the wall, enhanced wall treatment was used to model the boundary layer. This wall treatment predicts correct results for a broad range of normalized distances of the first cell to the wall.

3.4 Radiation

Radiation requires solving the radiative transfer equation (RTE). Here, we adopt the Discrete Ordinates Method (DOM), which discretizes the RTE in a number of directions

(4 θ-divisions, 2 ϕ-divisions). The gases are treated as grey gases, meaning that the spectral dependency is neglected.

3.5 Numerics

The conservation equations are discretized using first-order upwind for the convective terms, second-order central for the diffusive terms and backward Eulerian discretization for the time derivatives. A SIMPLE procedure is used to couple the equations.

4 COUPLING BETWEEN SOLID AND GAS PHASE

The coupling between the solid and gas phase solvers is done by solving the implicit system (4-5) with Gauss-Seidel iterations (fig. 3). More precisely, this means:

$$\begin{aligned} (\dot{\mathbf{q}}''_{in})^{n+1,k+1} &= G(\dot{\mathbf{m}}''_{pyr}, \mathbf{T}_s)^{n+1,k} \\ (\dot{\mathbf{m}}''_{pyr}, \mathbf{T}_s)^{n+1,k+1} &= S(\dot{\mathbf{q}}''_{in})^{n+1,k+1} \end{aligned} \tag{11}$$

The loop is considered to be converged if

$$\left\| (\dot{\mathbf{m}}''_{pyr}, \mathbf{T}_s)^{n+1,k+1} - (\dot{\mathbf{m}}''_{pyr}, \mathbf{T}_s)^{n+1,k} \right\| < 0.01 \tag{12}$$

where ||.|| means the L_2-norm of the vector.

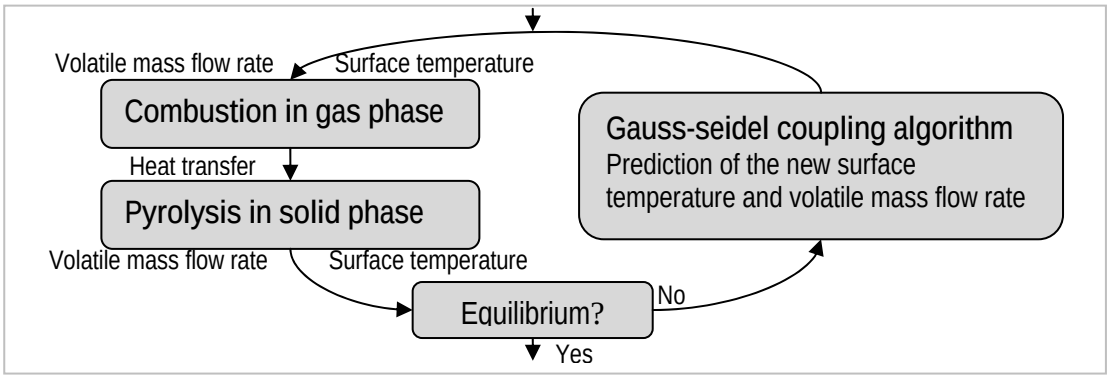

Figure 3: Coupling strategy between the combustion model and the pyrolysis model.

5 IGNITION AND DOWNWARD FLAME SPREAD

First, we simulate a laminar test case. A plate of PMMA, isolated at one side, is exposed to an external radiative heat flux. The incoming heat causes the material to pyrolyse. In the gas phase, a flame is not readily established once pyrolysis starts. It takes some time to ignite. The ignition delay time not only depends on the Arrhenius parameters of the reaction, but also on the behavior of the flow to obtain favorable circumstances for reaction (high temperature at a near stoichiometric mixture). Once a flame appears, it spreads in two directions. In this case, we are not interested in the upward flame spread behavior. Therefore, the radiation model was switched off. Focusing on the downward flame spread, a flame spread velocity could be obtained numerically.

Consider a gas phase calculation domain of 2 cm by 8 cm. At the bottom boundary, a constant uniform velocity is imposed. The top boundary is defined as a pressure-outlet. At the left boundary, symmetry conditions apply. The domain has a uniform mesh with grid size 0.4 mm. The right boundary is the solid PMMA material, which has a

thickness of 0.82 cm. The solid grid has a mesh size in y-direction equal to the gas phase. In x-direction, the solid is divided into 10 cells. The time step is taken equal to 0.01 seconds.

The external radiation is imposed at 2 cm below the top corner and has a Gaussian distribution with a width of 2 cm and a peak value of 50 kW/m^2.

For an inlet velocity of 0.3 m/s and an inlet temperature of 293 K, ignition takes place 5.6 seconds after radiation is switched on. A relatively big flame with high flame temperatures suddenly appears at the moment of ignition. From then on, the front moves slowly downwards at a speed of 0.08 mm/s.

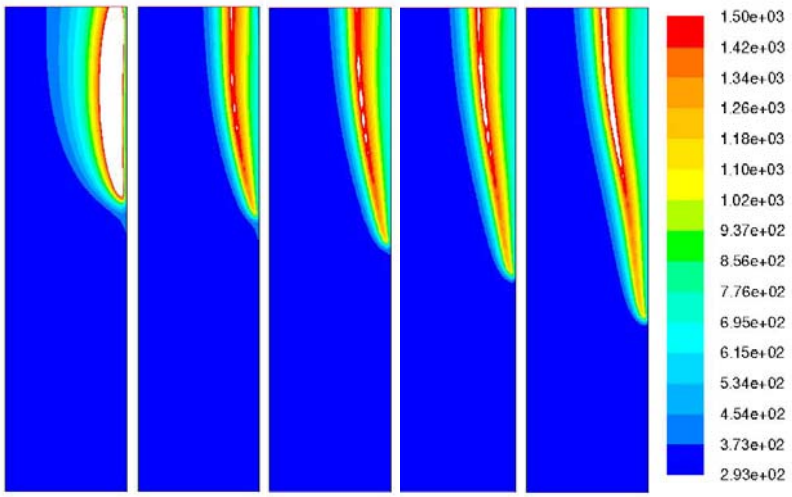

Figure 4: Downward flame spread (0.3 m/s, 293 K). Contours of temperature at 5.6 s, 10 s, 20 s, 40 s and 80 s

The given numerical results are only preliminary. A finer, non-uniform grid and higher-order discretizations will favor results that are more in line with e.g. [1]. Results for ignition delay times at different inlet temperatures and velocities are summarized in Table 1. The trend that ignition time increases with increasing velocity and decreasing temperature is confirmed also numerically. To illustrate that the phenomenon of downward flame spread is well captured, Fig. 4 shows contour plots of the temperature field at certain moments.

	0.7 m/s	**0.3 m/s**
293 K	5.9 s	5.6 s
340 K	4.3 s	4.1 s

Table 1: Ignition delay times as a function of inlet velocity and temperature.

6 UPWARD FLAME SPREAD

The upward flame spread test cases are simulated using a turbulence model. In this case, it is also important to take radiation heat fluxes into account.

In a first test case, we consider a charring solid of 3 mm thick and 10 cm high. This solid is exposed to an external constant heat flux of 40 kW/m^2 up to 6 mm high from the bottom. Initially, the entire set-up is at 295 K. The CFD-domain is 20 cm wide and 30

cm high. The solid interface is at the right boundary, which is composed of three pieces: the bottom and top 10 cm are treated as an adiabatic wall; the pyrolysing solid is placed in the middle 10 cm. The bottom, left and top boundaries of the CFD-domain are considered open. A pressure outlet boundary condition is applied, imposing a linearly varying pressure to incorporate the buoyancy. Where the pressure-outlet is in fact an inlet, the gas enters the domain normal to the boundary, having a turbulence intensity of 10% and a length scale based on a hydraulic diameter of 5 cm. A uniform Cartesian grid with spacing 2 mm is used in the gas phase. In the solid phase, the vertical grid spacing is 2 mm as well, resulting in a continuous grid at the interface. The grid spacing in horizontal direction is smaller (0.5 mm). The time step is equal to 0.1 s.

In the solid phase, we use the properties of white pine [6]: ρ_v=380.0 kg/m^3, ρ_c =76.0 kg/m^3, c_v =1196.0 J/kgK, c_c =986.8 J/kgK, k_v =0.36 W/mK, k_c =0.2 W/mK, Q_{pyr}=1.2 MJ/kg, T_{pyr}=658 K. The volatile gases are modeled as propane, with default properties.

Although the results differ somewhat from experimental observations, the coupling algorithm can be assessed because a flame appears, giving feedback to the solid material. Figure 5 shows the flame at t=50 s. Contours of temperature indicate that it takes some time for the fuel, generated at the surface exposed to external heat flux, to mix with the oxygen and react. Because of this artifact, a 'dead zone' of unburnt solid appears (fig. 6).

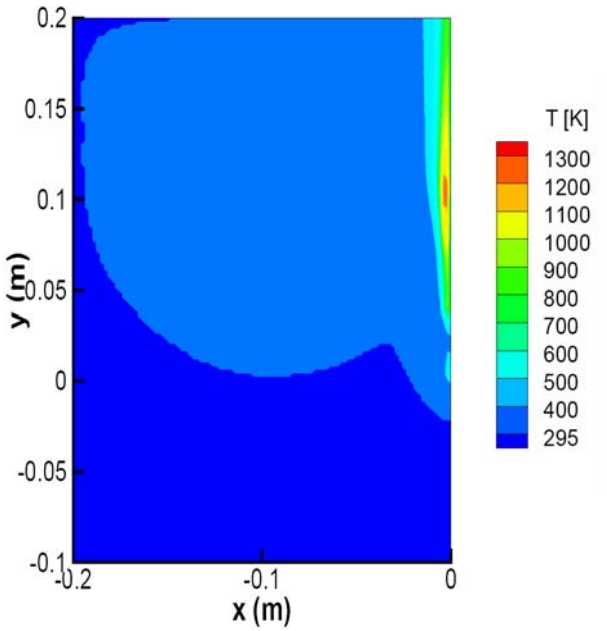

Figure 5: Upward flame spread. Contours of temperature at 50 s.

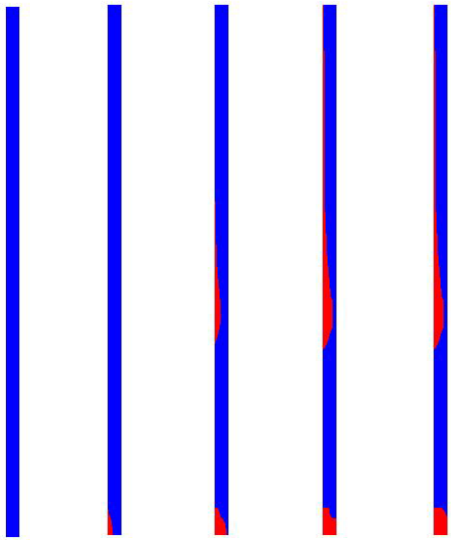

Figure 6: Char/virgin material distribution inside the solid at t=0 s, 50 s, 100 s, 150 s and 200 s.

A second test case consists of a non-charring material. The plate of pine wood in the above case is replaced by a plate of PMMA of 10 cm by 2.5 cm (similar to [2]). The horizontal grid spacing in the solid is 2.5 mm. An external heat flux of 50 kW/m^2 is applied at the bottom. A typical figure is provided in fig. 7. It is clear that the flame height is predicted far too long. More importantly, the leading edge of the flame appears too high, causing in this case no other material to pyrolyse than the part receiving the external heat flux. Numerical and modeling aspects, influencing the prediction of the flame's leading edge in the gas phase are the subject of the next paragraph.

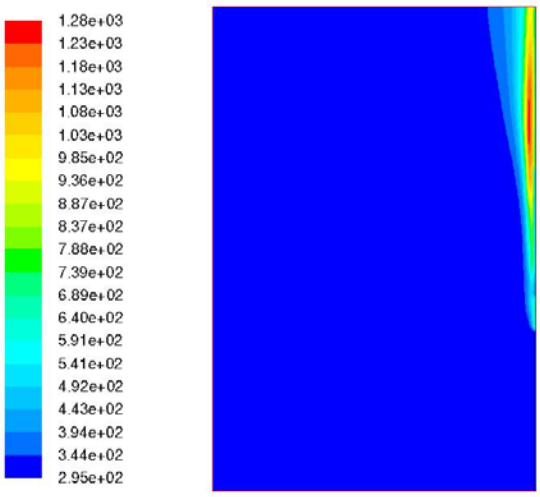

Figure 7: Upward flame spread for non-charring solid. Temperature contours reveal that the flame is predicted too high.

7 INFLUENCE OF TURBULENCE AND DISCRETIZATION

A correct prediction of the flame's leading edge is crucial to determine the right incident heat flux on the solid surface, which is the driving force for the upward flame spread phenomenon. The starting position of the flame fully depends on the reaction rate: higher reaction rates predict flame positions closer to the volatile inlet. Because the

Eddy Break-Up model is used to determine the reaction rates in case of a turbulent flow, the flame's position is determined by the turbulent quantities (k and ε). In this paragraph, different turbulence models are compared.

Since the coupling between gas and solid phase is not relevant for this investigation, no feedback from the flames is considered: the solid phase is modeled again as PMMA in the set-up of [2]; the solid has a uniform temperature of 630K (Pyrolysis temperature) and the bottom 10 cm of the 60cm high panel is considered to pyrolyse, releasing an amount of volatiles at a rate of 0.01 kg/m^2s. A 0.15m by 1.2m computational domain is considered. The PMMA-slab starts at 0.1m from the bottom and is 0.6m high. A non-uniform mesh with 60x460 cells is used. The distance of the nearest-wall node from the wall is 0.25mm whereas the distance between two nodes along the wall surface is 1mm for along the PMMA surface. The full right boundary is treated as a wall, which is isothermal in the PMMA-region and adiabatic in the other regions. The grid is almost identical to [2], but more extended to the left. The grid is made such that the y^+-value at the wall is around 1, advocating a low-Reynolds treatment.

Different two-equation turbulence models in Fluent were evaluated. For the k-ε-models (standard, realizable, RNG), enhanced wall treatment and buoyancy effects are included. k-ω-models (standard, SST) incorporate low-Reynolds effects. For a full description of the models, we refer to [7] and references therein.

Results with the different turbulence models are shown in figure 8 for two convective discretization schemes. The steady equations are solved until convergence is achieved. The fuel inlet is located in the interval [0, 0.1] at the right boundary. It can be observed for a first order upwind scheme (fig. 8, top) that there is little difference in the results obtained within the k-ε family. The standard k-ω model predicts the flame already at the beginning of the fuel inlet. The SST k-ω model shows no ignition.

Changing the discretization scheme from first order upwind to TVD (QUICK), does not change the overall picture (fig. 8, bottom), except for the SST k-ω model with low-Re corrections. In the latter case, no steady solution could be found. A more quantitative comparison between the different simulations is obtained by comparing the lowest position of the iso-contour of reaction rate (10^{-4} s^{-1}). It can be concluded from table 2 that in general, a higher order discretization results in a higher position of the flame. This can be understood, since less numerical dissipation is introduced. The general conclusion is true for k-ε models, but not for the k-ω models. In that case, sometimes a totally different result is obtained.

	standard k-ε	realizable k-ε	RNG k-ε	standard k-ω low Re corr	standard k-ω shearf low corr	standard k-ω low Re corr shear flow corr	sst k-ω lowRecorr	sst k-ω
1UPW	0.027	0.030	0.025	0.003	0.002	0.003	0.097	0.097
QUICK	0.044	0.045	0.041	0.003	0.002	0.049	-	-

Table 2: Lowest position (m) of iso-contour of reaction rate (10^{-4} s^{-1}).

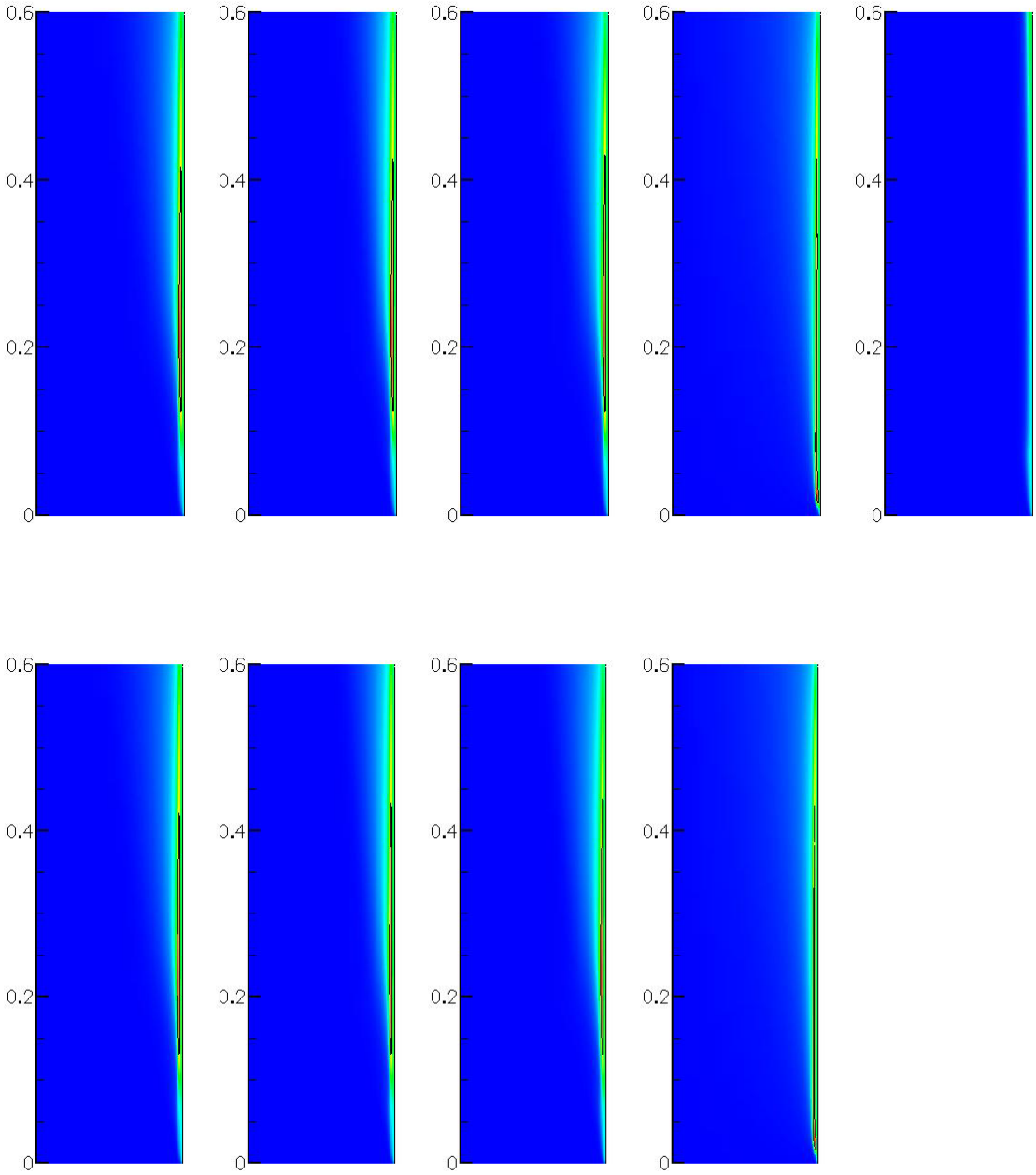

Figure 8: Influence of turbulence model and discretization on temperature field. From left to right: standard k-ε, realizable k-ε, RNG k-ε, standard k-ω with low-Re corrections and SST k-ω with low-Re corrections. Top: first order upwind, bottom: QUICK scheme. Contours of temperature vary from 295K to 1500K. The line indicates the 1000K isocurve.

8 CONCLUSION

In this paper, we described how the coupling between the gas phase and the solid phase is dealt with for the prediction of upward or downward flame spread. We chose to use two different simulation packages: a self-written code for the solid pyrolysis and a commercially available package for the gas phase combustion. The pyrolysis code has

the advantage that it uses a fixed mesh and can deal with both charring and non-charring materials. The use of a commercially available package has the advantage that it is well documented and organized and that it consists of many models and material properties. The coupling is stabilized with Gauss-Seidel iterations.

Two types of flame spread demonstrate the possibilities of this approach. The laminar downward flame spread simulation predicted good results, although some grid refinement studies are needed to be conclusive. The upward flame spread simulations were not satisfactory. The flame position, particularly the position of the leading edge of the flame, was wrongly predicted, causing the entire simulation result to be quantitatively incorrect. It was found that different turbulence models predict different flame positions. Especially, the k-ω type models are seen to be sensitive to variations in model parameters and discretization schemes. Better gas predictions are needed through grid refinements and extensions or even model changes. It was found, however, that the coupling between the two phases works fine, providing a mechanism of simulating flame spread with two different codes.

REFERENCES

[1] K.K. Wu, W.F. Fan, C.H. Chen, T.M. Liou and I.J. Pan, Downward flame spread over a thick PMMA slab in an opposed flow environment: experiment and modeling. *Comb. Flame* **132** , pp. 697–707 (2003).

[2] J.L. Consalvi, Y. Pizzo and B. Porterie, Numerical Analysis of the Heating Process in upward Flame Spread over thick PMMA slabs. *Fire Saf. J.* **43** , pp. 351-362 (2008).

[3] S.R. Wasan, P. Rauwoens, J. Vierendeels and B. Merci, Application of a simple Enthalpy-Based Pyrolysis Model in Numerical Simulations of Pyrolysis of Charring Materials". *Fire Mat.* **34** , pp. 39-54 (2010).

[4] S.R. Wasan, P. Rauwoens, J. Vierendeels and B. Merci, An Enthalpy-Based Pyrolysis Model for Charring and non-Charring Materials in Case of Fire. *Comb. Flame* **157** , pp. 715-734 (2010)

[5] J. West, L. Tang, R.A. Altenkirch, S. Bhattacharjee, K. Sacksteder and M.A. Delichatsios, Quiescent flame spread over thick fuels in microgravity. *Proc. Comb. Inst.* **26** , pp. 1335-1343 (1996).

[6] W.G. Weng and W.C. Fan, A pyrolysis model of charring materials considering the effect of ambient oxygen concentration. *Fire Mat.* **31** , pp. 463-475 (2007).

[7] Fluent 12.0 Theory Guide.